Calculation of Thermoelectric Properties of Doped $SrTiO_3$

T. Chanapote* and A. Yangthaisong
Computational Materials and Device Physics Group, Department of Physics,
Faculty of Science, Ubon Ratchathani University, Ubonratchathani, 34190, Thailand
**Corresponding Author: t.chanapote@gmail.com, Tel: 086-8657805*

Abstract

Thermoelectric properties of cubic perovskite $SrTiO_3$ have been investigated. The energy band structures are calculated using the total energy plane-wave pseudopotential method within the local density approximation (LDA) and generalized gradient approximation (GGA). The calculated energy band structures are then used in combination with Boltzmann transport equation to calculate the thermoelectric parameters of doped $SrTiO_3$ especially seebeck coefficient, electrical conductivity and electronic thermal conductivity.

Keywords: $SrTiO_3$, Density functional theory, Boltzmann transport equation, Thermoelectric properties.

1. Introduction

Thermoelectric devices have gained interest as a power generation because it can generate electricity from waste heat and could play an important role in a global sustainable energy solution[1]. Thermoelectric materials convert thermal energy directly to electrical energy via Seebeck effect by temperature difference in solid materials[2]. An interesting application is the recovery of energy from exhaust gas of vehicles. In conventional vehicles driven by internal combustion engines approximately one third of the energy content of the fuel is dissipated as waste heat in the exhaust gas stream and this dissipation is at high temperature that in principle could be recovered by using thermoelectrics, based on thermodynamic limits. Therefore it can improve energy utilization efficiency and reduce CO_2 emission. The conversion performance of thermoelectric materials can be accessed through dimensionless figure of merit, ZT :

$$ZT = TS^2\sigma / \kappa \qquad (1)$$

where T is the temperature, S is the Seebeck coefficient, σ is the electrical conductivity and κ is the thermal conductivity[3].

The materials owning perovskite strcutures exhibit a number of attractive properties such as ferroelectric[4], piezoelectric[5], magnetic, catalytic[6], ionically conductivity[7], and thermoelectric properties[8]. Recently, several perovskite-type oxides have been studied for high temperature thermoelectric materials. Among them a single crystal of (Sr, La)TiO_3 has been reported to have a high power factor comparable to that of Bi-Te alloy at room temperature [9]. Besides, a large power factor of $2\text{-}3\times10^{-3}$ W/m.K^2, comparable to that of traditional thermoelectric material Bi_2Te_3[9], has been demonstrated in bulk $SrTiO_3$[10]. Nonetheless, due to its high thermal conductivity of about 10 W/m.K, the dimensionless conversion performance is only 0.1. To enhance the thermoelectric performance of $SrTiO_3$, ion substitution approach has been proposed and investigated intensively both theoretically and experimentally[11]. In fact, electron-doped $SrTiO_3$ can be considered to as an appropriate n-type oxide for high temperature thermoelectric applications[12].

The main purpose of this study is to investigate the thermoelectric properties of $SrTiO_3$ at various doping levels and temperatures by first principles calculations and Boltzmann transport equation. The calculated results obtained will be compared with the experiment.

2. Materials and Methods

2.1 Material Structure

The materials being studied in this paper is cubic perovskite $SrTiO_3$. Its unit cell contains five atoms: one Ti atom at the cubic center, One Sr atom at the cube corner and three O atoms at the face center as illustrated in Fig. 1.

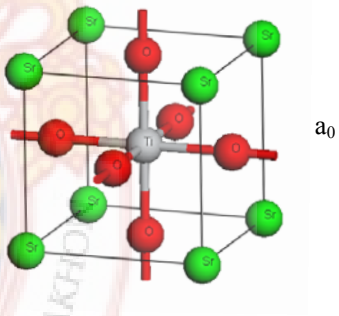

Fig. 1 The cubic structure of perovskite-type $SrTiO_3$.

2.2 Computational Methods

a) Electronic structure

The electronic structures have been calculated by first principle method based on plane-wave pseudopotential density functional theory(DFT), as implemented in CASTEP code[13]. Vanderbilt ultra-soft pseudopotential within the CA-PZ form are employed[14]. Only

valence electrons are taken into account and represented as $Sr(4s^24p^65s^2)$, $Ti(3d^26s^2)$ and $O(2s^22p^4)$. electronic exchange and correlation effects were described by local density approximation (LDA), generalized gradient approximation (GGA). The geometry optimization is determined using Broyden-Fletcher-Goldfarb-Shenno (BFGS) minimization technique, with the threshold for converged structure: energy change per atom less than 1×10^{-5} eV/atom, residual force less than 0.03 eV/Å, stress below 0.05 GPa and the displacement of atoms during the geometry optimisation less than 0.001 Å. The tolerance in the self-consistent field (SCF) calculation is 1×10^{-6} eV/atom. Plane wave cut-off energy of 340 eV and a $6\times6\times6$ Monkhorst-Pack k-point mesh have been used for the Brillouin zone integration to ensure well convergence of the computed structure and energies.

b) Thermoelectric coefficients

To predict thermoelectric properties of materials, the BolzTraP program based on Boltzmann theory developed by D. J. Singh 's group[15] has been modified and used in this work. The diagram of our approach is illustrated in Fig. 2. Technically, by using the calculated band structure in conjunction with the Boltzmann transport equation and the rigid band approach as described in details in [15], the conductivity of material is based on the transport distribution

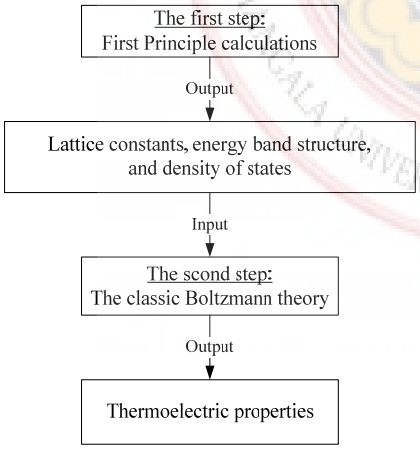

Fig. 2 Diagram of calculations

$$\sigma_{\alpha\beta}(\varepsilon)=\frac{1}{N}\sum_{i,k}\sigma_{\alpha\beta}(i,k)\frac{\delta(\varepsilon-\varepsilon_{i,k})}{d\varepsilon} \quad (2)$$

Hence, the transport tensors can then be calculated from the conductivity distributions:

$$\sigma_{\alpha\beta}(T,\mu)=\frac{1}{\Omega}\int\sigma_{\alpha\beta}(\varepsilon)\left[-\frac{\partial f_\mu(T;\varepsilon)}{\partial\varepsilon}\right]d\varepsilon \quad (3)$$

$$\upsilon_{\alpha\beta}(T;\mu)=\frac{1}{eT\Omega}\int\sigma_{\alpha\beta}(\varepsilon)(\varepsilon-\mu)\left[-\frac{\partial f_\mu(T;\varepsilon)}{\partial\varepsilon}\right]d\varepsilon) \quad (4)$$

$$\kappa^0_{\alpha\beta}(T;\mu)=\frac{1}{e^2T\Omega}\int\sigma_{\alpha\beta}(\varepsilon)(\varepsilon-\mu)^2\left[-\frac{\partial f_\mu(T;\varepsilon)}{\partial\varepsilon}\right]d\varepsilon \quad (5)$$

where κ_0 is the electronic part of the thermal conductivity, $\upsilon_{\alpha\beta}$ is the group velocity, f is the Fermi-Dirac distribution function, T is absolute temperature, and μ is chemical potential. It is worthwhile to mention that in the rigid band approach, the bands and hence $\sigma(\varepsilon)$ are left fixed. This means that only band structure calculations are required, simplifying the calculations. To further simplify the problem, one can also assume that Seebeck coefficient(S) is independent of relaxation time (τ), hence it can be written as $S=\sigma^{-1}\upsilon$. Eventually, the calculated Seebeck coefficients and electrical conductivities are then used to predict thermoelectric power factor ($PF = S^2\sigma$). Note the electronic thermal conductivity at zero electric current can be calculated using the following expression:

$$\kappa^e_{ij}=\kappa^0_{ij}-T\upsilon_{i\alpha}(\sigma^{-1})_{\beta\alpha}\upsilon_{\beta j} \quad (7)$$

3. Results and discussions

3.1 Electronic structure

The lattice constants from geometry optimization are 3.87 Å and 3.95 Å for LDA, GGA calculations, respectively while the experimental value is 3.89 Å [16].

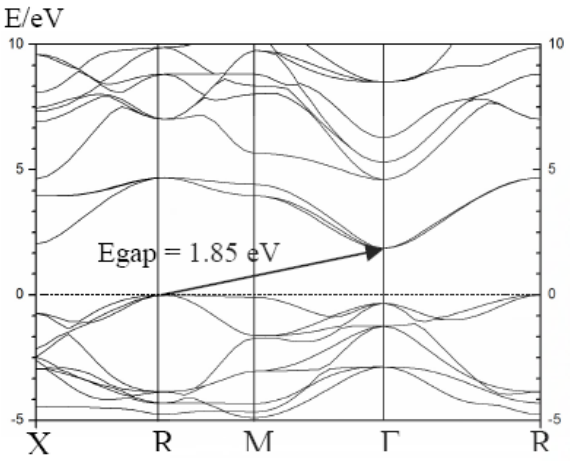

Fig. 3 The LDA electronic structure of $SrTiO_3$.

Fig. 3 shows the LDA electronic structure of $SrTiO_3$. It can be seen that $SrTiO_3$ is a semiconductor with indirect energy gap 1.85 eV. A similar pattern with the gap of 1.83 eV was obtained for GGA calculation(not shown). Our calculations agree with other recent calculations[11]. It is worthwhile to mention here that the energy gaps calculated from density functional theory with LDA(GGA) underestimate the experimental gaps seems to be a known artifact of the LDA(GGA) methods[17]. The methods beyond the LDA with give correct band gap are required. These calculations include GW approximation[18], B3LYP[19], LDA plus U[20], screened exchange (sX)[21], and weighted density approximation (WDA)[22]. It is very instructive to investigate further and in fact, our calculations utilizing sX is being studied and will be reported elsewhere. In this work, we correct this problem by an empirical upward shift of the conductional band to the experiment value of 3.25 eV[23] to obtain more realistic thermoelectric properties.

3.2 Thermoelectric coefficients

The calculated Seebeck coefficient as a function of electron concentration is plotted at various temperatures in Fig. 4(a). It can be seen that Seebeck coefficients decrease with the increasing electron concentrations but increase with the increasing temperatures. On the other hand, the electrical conductivity with respect to the relaxation time is quite independent of temperature but very much dependent on electron concentrations as shown in Fig. 4(b). Hence, the power factor per relaxation time increases with increasing temperature but it is quite independent of electron concentration at a wide range as shown in Fig. 4(c).

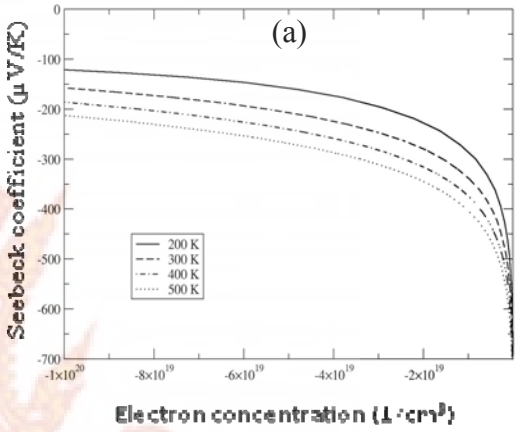

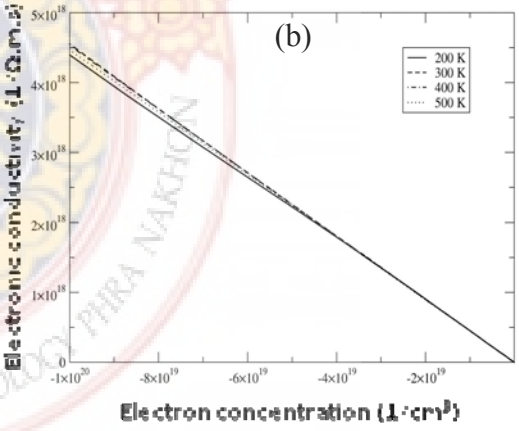

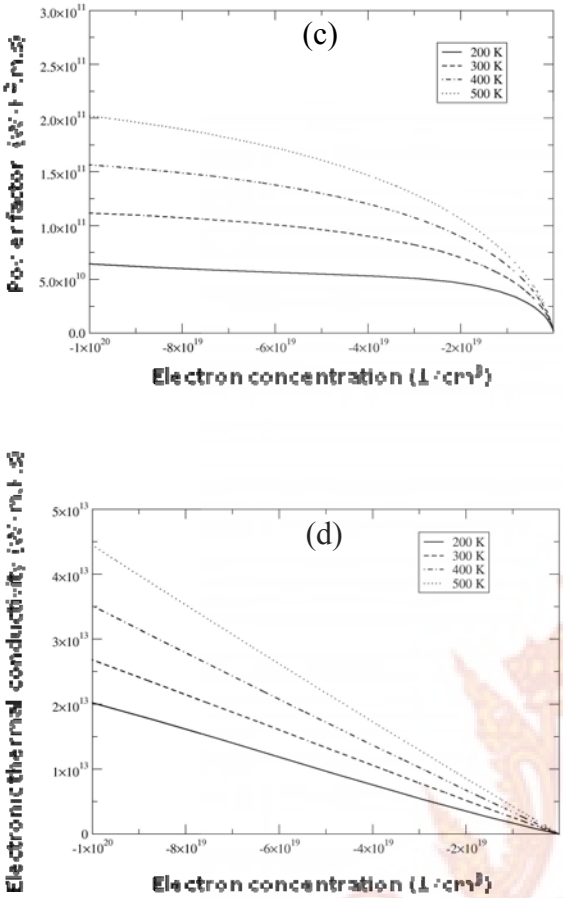

Fig. 4 (a) Seebeck coefficient (b) Electrical conductivity (c) Power factor and (d) Electronic thermal conductivity of $SrTiO_3$

The calculated electronic thermal conductivity increases with both the increasing temperature and electron concentration as shown in Fig. 4(d). This is consistent with Wiedemann-Franz law.

To compare our predictions with available data reported in [10], Seebeck coefficient and electron conductivity are plotted as a function of electron concentration at 300 K. Fig. 5 shows that our calculated Seebeck coefficients are about half of experiment values. Nonetheless, our predictions can capture the trend found in experiment. The calculated electrical conductivity as a function of electron concentration is shown in Fig. 5(b). Note that the relaxation time constant (τ) 0.1×10^{-14} s was employed. Due to many effects, thermoelectric parameters from the calculations and the experiments are not the same as seen in Fig. 5 a) in case of the Seebeck coefficient. For the most important one, the band structure used in this study was calculated in the condition of absolute zero temperature which in general is temperature dependent.

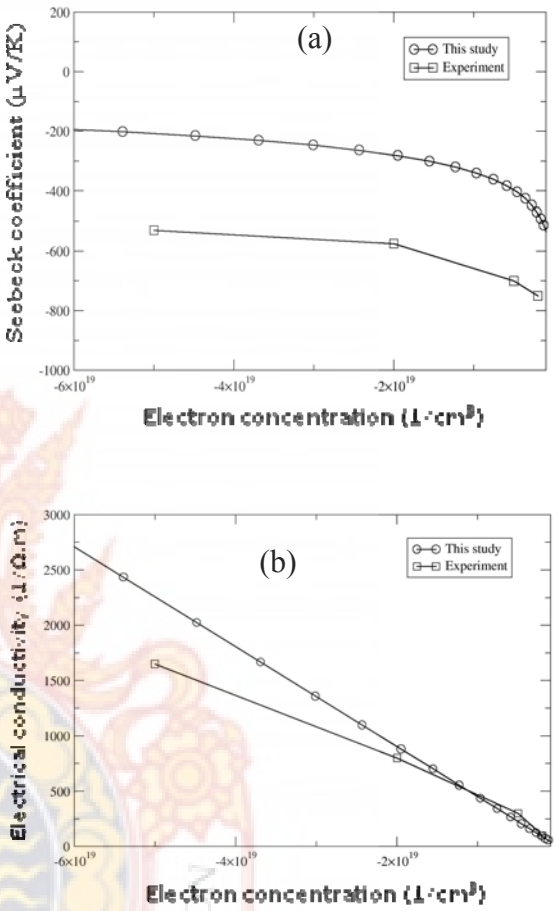

Fig. 5 (a) Seebeck coefficient (b) Electrical conductivity of $SrTiO_3$ compared with the experiment.

4. Conclusions

The thermoelectric properties of $SrTiO_3$ were studied by first principles calculation together with Boltzmann transport equation. It is found that Seececk coefficient decreases with increasing electron concentration and increases with increasing temperature. The electrical conductivity is independent with temperature but increases with increasing electron

concentration. The electric thermal conductivity increases with both increasing temperature and electron concentration.

5. Acknowledgements

The work described in this paper has been supported by National Research council (Grant No. 2553A11702048). This work has partially been supported by the National Nanotechnology Center (NANOTEC), National Science and Technology Development Agency, through its Computational Nanoscience Consortium (CNC). A. Y. acknowledges Dr. S. J. Clark, Durham University, UK for providing his code. The computing resources through SILA clusters at Ramkhamhaeng University are very grateful.

6. References

[1] Hongxia Xi et. al. 2007. Development and applications of solar-based thermoelectric technologies. Renewable and Sustainable Energy Review. 11 : 923 – 936.

[2] Basel I. Ismail and Wael H. Ahmed. 2009. Thermoelectric Power Generation Using Waste-Heat Energy as an Alternative Green Technology. Recent Patents on Electrical Engineering. 2 : 27-39

[3] T.J. SCHEIDEMANTEL et al. 2003. Thermoelectric coefficient from First-principles calculations. Physical Review B. 68. 125210.

[4] Bee Keen Gan and Kui Yao. 2009. Structure and enhanced properties of perovskite ferroelectric PNN–PZN–PMN–PZ–PT ceramics by Ni and Mg doping. Ceramics International. 35 : 2061–2067.

[5] Yi Chen et. al. 2008. Bismuth-modified BiScO3–PbTiO3 piezoelectric ceramics with high Curie temperature. Materials Letters. 62 : 3567–3569.

[6] Hirohisa Tanaka et. al. 2003. Catalytic activity and structural stability of La0.9Ce0.1Co1−*x*Fe*x*O3 perovskite catalysts for automotive emissions control. Applied Catalysis A: General. 244 : 371–382.

[7] H. Hayashi et. al. 1999. Structural consideration on the ionic conductivity of perovskite-type Oxides. Solid State Ionics. 122 : 1–15.

[8] Takuji Maekava et. al. 2005. Thermoelectric properties of perovskite type strontium ruthenium oxide. Journal of Alloys and Compounds. 387 : 56–59.

[9] T. Okuda, K. Nakanishi, S.Miyasaka, Y. Tokura. 2001. Large thermoelectric response of metallic perovskites: $Sr_{1-x}La_xTiO_3$ ($0 \leq x \leq 0.1$). Physical Review B. 63. 113104.

[10] Jun Okamoto et al. 2009. Thermoelectric properties of B-doped SrTiO3 single crystal. Journal of Physics: Conference Series. 176. 012042.

[11] J. C. Li et. al. 2008. Electronic structure and thermoelectric properties of Fe-doped BaTiO2 and SrTiO3. IEEE. 978 : 175 – 178

[12] Hiroaki Muta et.al. 2003. Thermoelectric properties of rare earth doped $SrTiO_3$. Journal of Alloys and Compounds 350 : 292 – 295.

[13] Stewart J. Clark et al. 2005. First principles methods using CASTEP. Zeitschrift für Kristallographie. 220 : 567 – 570.

[14] D.Vanderbilt. 1990. Soft self-consistent pseudopotentials in a generalized eigenvalue formalism. Physical Review B. 41. 7892.

[15] G.K.H. Madsen and D.J. Singh. 2006. BoltzTraP. A code for calculating band-structure dependent quantities. Computer Physics Communications. 175 : 67 – 71.

[16] K.H. Hellwage, A.M. Hellwege (Eks.), 1969. Ferroelectrics and Related Substances, New Series, vol. 3, Landolt-Bornstein, *Springer Verlag, Berlin, group III.*

[17] J.P. Perdew and A. Zunger, 1981. Self-interaction correction to density-functional approximations for many-electron systems. Physical Review B. 23. 5040.
[18] F. Aryasetiawany and O. Gunnarssonz. 1998. The *GW* Method. Reports on Progress in Physics. 61 : 237 – 312
[19] Th. Dittrich et. al. 2004. Photovoltage characterization of $CuAlO_2$ crystallites. Applied Physics Letters. 85(5) : 742 - 744.
[20] R. Dovesi et. al. 2000. The Periodic Hartree-Fock Method and Its Implementation in the Crystal Code. Physica Status Solidi (b). 217 : 63 – 88.
[21] V.I. Anisimov et. al. 1991. Density-functional calculation of effective coulomb interactions in metals. Physical Review B. 44(3) : 943 – 954.
[22] B.M. Bylander and L. Kleinman. 1990. Good semiconductor band gaps with a modified local-density approximation. Physical Review B. 41(11) : 7861-7871.
[23] K. van Benthem, C. Elsasser, R.H. French. 2001. Bulk electronic structure of SrTiO3 : Experiment and theory. Journal of Applied Physics. 90(12). 6156.